Arthritis & Rheumatology
Vol. 74, No. 5, May 2022, pp 892–901
DOI 10.1002/art.42043

American College of Rheumatology
Empowering Rheumatology Professionals

CD163+ M2 Macrophages Promote Fibrosis in IgG4-Related Disease Via Toll-like Receptor 7/Interleukin-1 Receptor–Associated Kinase 4/NF-κB Signaling

Akira Chinju,[1] Masafumi Moriyama,[1] Noriko Kakizoe-Ishiguro,[1] Hu Chen,[1] Yuka Miyahara,[1] A. S. M. Rafiul Haque,[2] Katsuhiro Furusho,[3] Mizuki Sakamoto,[1] Kazuki Kai,[1] Kotono Kibe,[4] Sachiko Hatakeyama-Furukawa,[1] Miho Ito-Ohta,[1] Takashi Maehara,[1] and Seiji Nakamura[1]

Objective. IgG4-related disease (IgG4-RD) is a fibro-inflammatory condition that can affect multiple organs. We previously demonstrated that *TLR7*-transgenic C57BL/6 mice showed elevated serum IgG1 levels and inflammation with fibrosis in the salivary glands (SGs), lungs, and pancreas. Moreover, we observed extensive Toll-like receptor 7 (TLR-7)–positive CD163+ M2 macrophage infiltration in SGs from IgG4-RD patients. We undertook this study to examine the fibrotic mechanism via the TLR-7 pathway.

Methods. Gene expression in SGs from human *TLR7*-transgenic mice and IgG4-RD patients was analyzed using DNA microarrays. We extracted the common up-regulated TLR-7–related genes in SGs from *TLR7*-transgenic mice and IgG4-RD patients. Finally, we investigated the interaction between CD163+ M2 macrophages and fibroblasts before and after stimulation with the TLR-7 agonist loxoribine.

Results. In *TLR7*-transgenic mice and IgG4-RD patients, *IRAK3* and *IRAK4* were significantly overexpressed. Real-time polymerase chain reaction validated the up-regulation of only *IRAK4* in IgG4-RD patients compared with the other groups ($P < 0.05$). Interleukin-1 receptor–associated kinase 4 (IRAK4) was strongly detected in and around germinal centers in SGs from patients with IgG4-related dacryoadenitis and sialadenitis alone. Double immunofluorescence staining showed that IRAK4-positive cells were mainly colocalized with CD163+ M2 macrophages in SGs ($P < 0.05$). After stimulation with loxoribine, CD163+ M2 macrophages exhibited significantly enhanced expression of IRAK4 and NF-κB and increased supernatant concentrations of fibrotic cytokines. Finally, we confirmed that the number of fibroblasts was increased by culture with the supernatant of CD163+ M2 macrophages following stimulation with loxoribine ($P < 0.05$).

Conclusion. CD163+ M2 macrophages promote fibrosis in IgG4-RD by increasing the production of fibrotic cytokines via TLR-7/IRAK4/NF-κB signaling.

INTRODUCTION

IgG4-related disease (IgG4-RD) is an immune-mediated systemic condition affecting various organs including the lacrimal glands, submandibular glands (SMGs), kidneys, lungs, thyroid, liver, bile ducts, pancreas, prostate, aorta, lymph nodes, and mammary glands (1–3). Increased serum IgG4 levels and sclerosing changes with abundant IgG4-positive plasma cells and severe fibrosis are the main clinical features of IgG4-RD (4).

Although the pathogenic involvement of adaptive immune responses mediated by T helper cells and plasmablasts in IgG4-RD is well established (5–12), recent studies have highlighted the innate immune responses underlying the immunopathogenesis of IgG4-RD (13–15). We previously confirmed the

Supported by the Ministry of Education, Culture, Sports, Science, and Technology of Japan (grants 21H03141 and 20H00553) and the Ministry of Health, Labour and Welfare Research Program on Rare and Intractable Diseases (grant JPMH20FC1040).

[1]Akira Chinju, DDS, Masafumi Moriyama, DDS, PhD, Noriko Kakizoe-Ishiguro, DDS, PhD, Hu Chen, DDS, Yuka Miyahara, DDS, Mizuki Sakamoto, DDS, Kazuki Kai, DDS, Sachiko Hatakeyama-Furukawa DDS, PhD, Miho Ito-Ohta, DDS, PhD, Takashi Maehara, DDS, PhD, Seiji Nakamura, DDS, PhD: Kyushu University, Fukuoka, Japan; [2]A. S. M. Rafiul Haque, DDS, PhD: Udayan Dental College, Rajpara, Bangladesh; [3]Katsuhiro Furusho DDS, PhD: National Center for Geriatrics and Gerontology, Aichi, Japan; [4]Kotono Kibe, DDS: Kyushu University, Fukuoka, Japan, and University of Tokyo, Tokyo, Japan.

Author disclosures are available at https://onlinelibrary.wiley.com/action/downloadSupplement?doi=10.1002%2Fart.42043&file=art42043-sup-0001-Disclosureform.pdf.

Address correspondence to Masafumi Moriyama, DDS, PhD, Section of Oral and Maxillofacial Oncology, Division of Maxillofacial Diagnostic and Surgical Sciences, Faculty of Dental Science, Kyushu University, 3-1-1 Maidashi, Higashi-ku, Fukuoka 812-8582, Japan. Email: moriyama@dent.kyushu-u.ac.jp.

Submitted for publication June 15, 2021; accepted in revised form December 7, 2021.

extensive infiltration of M2 macrophages expressing CD163 in salivary glands (SGs) from patients with IgG4-RD, which indicates that M2 macrophages contribute to tissue fibrosis via the production of profibrogenic factors, including CCL18 and interleukin-10 (IL-10) (16), as well as the activation of Th2 immune responses via IL-33 secretion (17). Moreover, recent studies have indicated that Toll-like receptors (TLRs), which are important for innate immunity, are associated with the pathogenesis of IgG4-RD (18–20). Fukui et al examined the number of TLR-1–TLR-11–positive cells in pancreatic tissues from IgG4-related autoimmune pancreatitis (AIP) patients (21). The ratio of TLR-7–positive monocytes/macrophages to infiltrated monocytes/macrophages was significantly higher in type 1 AIP patients.

We also reported the accumulation of TLR-7–positive CD163+ M2 macrophages in SMGs from patients with IgG4-RD (17). Interestingly, our recent data confirmed that *TLR7*-transgenic/TLR-7$^{-/-}$ mice exhibited a phenotype similar to that of IgG4-RD patients. Specifically, fibro-inflammation in the SMGs, pancreas, and lungs was shown in *TLR7*-transgenic/TLR-7$^{-/-}$ mice compared with wild-type mice. In addition, serum concentrations of IgG, IgG1 (equivalent to human IgG4), and IL-33 in *TLR7*-transgenic/TLR-7$^{-/-}$ mice were markedly increased following stimulation with a TLR-7 agonist. This indicated that TLR-7 signaling is associated with the pathogenesis of IgG4-RD (22). However, it remains unknown why *TLR7*-transgenic/TLR-7$^{-/-}$ mice exhibit a phenotype similar to IgG4-RD patients. Here, we investigated the downstream events of TLR-7 signaling in *TLR7*-transgenic/TLR-7$^{-/-}$ mice and IgG4-RD patients to clarify the fibrotic mechanism that contributes to IgG4-RD.

PATIENTS AND METHODS

Study participants. The study protocol was approved by the accredited Medical Ethical Committees of Kyushu University Hospital (approval nos. 25-287 and 26-86). All patients provided written informed consent prior to participation. The study was conducted in accordance with the ethical principles of the Declaration of Helsinki and the approved guidelines of Kyushu University Hospital.

Peripheral blood and SGs were obtained from patients with IgG4-RD (n = 15), those with primary Sjögren's syndrome (SS) (n = 15), and those with chronic sialadenitis (CS) (n = 15), as well as healthy controls (n = 15) recruited from the Department of Oral and Maxillofacial Surgery at Kyushu University Hospital, between 2012 and 2020. Details on the clinical profiles of the IgG4-RD patients are available in Supplementary Table 1 (available on the *Arthritis & Rheumatology* website at https://onlinelibrary.wiley.com/doi/10.1002/art.42043). Healthy donors were defined by a lack of any current history or history of malignancy, autoimmune disease, or chronic infections.

We performed labial SG biopsy and open SMG incisional biopsy in patients with IgG4-RD and those with primary SS, as previously described (23), and SG extraction in CS patients. IgG4-RD was diagnosed according to the 2020 Revised Comprehensive Diagnostic Criteria for IgG4-Related Disease (24) and the Diagnostic Criteria for IgG4-related dacryoadenitis and sialadenitis (IgG4-DS) (25). All patients with IgG4-RD showed typical histopathologic findings, including marked infiltration of IgG4-positive plasma cells, severe fibrosis, and formation of multiple ectopic germinal centers (GCs), and had not received previous treatment with steroids or other immunosuppressants. SS was diagnosed according to the 1999 Research Committee on SS of the Ministry of Health, Labour and Welfare of the Japanese Government (26) and the American College of Rheumatology/European Alliance of Associations for Rheumatology 2016 classification criteria for primary SS (27).

All patients with SS exhibited lymphocytic infiltration in SGs, had no other autoimmune diseases, and had not received previous treatment with steroids or other immunosuppressants. There was no documented history of HIV, human T cell lymphotropic virus type 1, hepatitis B virus, or hepatitis C virus infection in any of the patients. None of the patients had evidence of malignant lymphoma at the time of the study. As a comparative healthy sample, SGs, tonsils, and lymph nodes were obtained from patients with oral squamous cell carcinoma (OSCC) at tumor resection. These samples from OSCC patients were histologically normal and lacked clinical evidence of metastasis or radiation therapy, and were defined as healthy controls.

Gene expression microarrays. Complementary RNA was amplified and labeled using a Low Input Quick Amp Labeling Kit, in accordance with instructions of the manufacturer (Agilent Technologies) and hybridized to SurePrint G3 Human Gene Expression Microarrays 8 60K version 2 (DNA chip including 60,000 genes; Agilent Technologies). All hybridized microarray slides were scanned using an Agilent scanner. Relative hybridization intensities and background hybridization values were calculated using Agilent Feature Extraction Software (version 9.5.1.1), as previously described (28).

Real-time quantitative polymerase chain reaction (PCR). Total RNA was isolated from SGs using an RNeasy RNA extraction kit (Qiagen), and complementary DNA (cDNA) was synthesized as previously described (29). The resulting cDNA was amplified using the PowerUp SYBR Green Master Mix (ThermoFisher Scientific) in an AriaMx Real-Time PCR instrument (version 1.7; Agilent Technologies). The levels of messenger RNA (mRNA) for *TLR7, IRAK3, IRAK4, MyD88, IRF5, IRF7, TRAF6, NFKB, ACTA2,* and *FAP* were analyzed. The relative mRNA levels were calculated after normalizing to the housekeeping gene β-actin. The primer sequences used are described in the Supplementary Methods (available on the *Arthritis & Rheumatology* website at https://onlinelibrary.wiley.com/doi/10.1002/art.42043). All analyses were performed in triplicate.

Immunohistochemical analysis. SG samples were cut into 4-μm–thick formalin-fixed and paraffin-embedded sections, and immunohistochemical staining was performed for CD11c, CD80, CD123, CD163, interleukin-1 receptor–associated kinase 3 (IRAK3), and IRAK4, as previously described (23). Details of the antibodies used in this study are shown in Supplementary Table 2 (available on the *Arthritis & Rheumatology* website at https://onlinelibrary.wiley.com/doi/10.1002/art.42043). Hematoxylin and eosin counterstaining was performed after immunohistochemical staining. For multi-immunofluorescence analyses, the 4-μm–thick histologic sections of SGs were stained with anti-CD163, anti-CD123, anti-CD11c, anti-IRAK4, and anti-CD80 antibodies using an Opal 4-Color Manual IHC Kit (catalog no. NEL810001KT; PerkinElmer), and analyzed under a light microscope (IX83; Olympus Corporation).

Quantitative image analysis. TissueQuest software (TissueGnostics) provides automated high-resolution imaging with the scientific accuracy of flow cytometry (http://www.bga.su/info/TissueFAXS). Stained cells were automatically counted in the SG specimens. Staining of SG specimens was quantified using TissueQuest software, with cutoff values determined relative to the positive controls, as previously described (7).

Evaluation of the severity of fibrosis. Masson's trichrome staining uses 3 stains to selectively identify fibrotic areas (blue), nuclei (dark brown), and cytoplasm (red). The fibrosis score was calculated from the ratio of the fibrotic area to the whole stained area in a 4-μm^2 field of view, from 5 different areas.

In vitro experiments. CD163+ M2 macrophages were isolated from healthy peripheral blood mononuclear cells as described in a previous report (22), and were then stimulated with 500 μ*M* of the TLR-7 agonist loxoribine (catalog no. ALX-480-097-M025; Enzo Life Sciences) and/or 1 μ*M* of the IRAK4 inhibitor CA-4948 (Selleck) (Supplementary Figures 1 and 2, available on the *Arthritis & Rheumatology* website at https://onlinelibrary.wiley.com/doi/10.1002/art.42043). Supernatants and RNA were collected for further analysis.

In vivo experiments. To examine the in vivo function of *TLR7*, we established TLR-$7^{-/-}$ mice and *TLR7*-transgenic/TLR-$7^{-/-}$ mice on a C57BL/6 background, as described in a previous report (22). For the *TLR7* ligand treatment of transgenic mice, their ear skin was topically treated 3 times per week with 100 μg of resiquimod (R848; ChemScene Chemicals) in 100 μl of acetone.

Additional details. Reagents and more detailed methods for the isolation of CD163+ M2 macrophages, establishment of transgenic mice, flow cytometry analysis, enzyme-linked immunosorbent assay, cell proliferation assay, and cell division assay are described in the Supplementary Methods and Supplementary Figures 1 and 2 (available on the *Arthritis & Rheumatology* website at https://onlinelibrary.wiley.com/doi/10.1002/art.42043).

Statistical analysis. Data are presented as the mean ± SD. Student's *t*-test, Mann–Whitney U-test, chi-square test, Kruskal–Wallis test, and Spearman's rank correlations were used to calculate the statistical significance of differences between groups. *P* values less than 0.05 were considered statistically significant. All analyses were performed using GraphPad Prism 9.

RESULTS

Phenotype of *TLR7*-transgenic/TLR-$7^{-/-}$ mice. As mentioned above, we established *TLR7*-transgenic/TLR-$7^{-/-}$ mice as a model of IgG4-RD. To confirm the phenotype of transgenic mice, 4-week-old transgenic and knockout mice were stimulated with a TLR-7 agonist (R848) for 4 weeks (Figure 1A). Histologic and serologic examinations were performed, with transgenic and knockout mice treated with the TLR-7 agonist. Representative histologic findings in the SMGs from transgenic and knockout mice are shown in Figure 1B. The degree of lymphocytic infiltration in the SMGs from transgenic mice was markedly increased compared with that in the SMGs from knockout mice. Moreover, we evaluated the degree of fibrosis in SMGs specimens by Masson's trichrome staining. The fibrosis scores in the SMGs from transgenic mice were significantly higher than those in the SMGs from knockout mice (Figure 1C).

Furthermore, transgenic mice had significantly high levels of serum IgG and IgG1 after TLR-7 agonist stimulation compared with knockout mice (Figure 1D). Murine IgG1 is considered to be functionally equivalent to human IgG4.

Gene expression profiles of TLR-7–related and fibrosis-related genes in SMGs from transgenic mice. Gene expression profiling by DNA microarray was performed to evaluate the differences in gene expression of SMG samples between transgenic and knockout mice. The heatmap for TLR-7–related and fibrosis-related genes is shown in Figure 1E. The expression levels of the TLR-7–related genes, *Irf5, Irak3,* and *Irak4*, were significantly increased in transgenic mice compared with knockout mice. In addition, Figure 1F shows a heatmap demonstrating the differences in TLR-7–related and fibrosis-related gene expression levels between IgG4-RD patients and healthy controls. The expression levels of the TLR-7–related genes, *IRF3, IRF5, IRF7, TRAF6, IRAK3, IRAK4,* and *MyD88*, were significantly higher in IgG4-RD patients compared with healthy controls. Thus, we focused on *Irak3*, *Irak4*, and *IRF5*, which are commonly up-regulated TLR-7–related genes in transgenic mice and IgG4-RD patients. The validation of the real-time PCR for the detection of these common TLR-7–related candidate

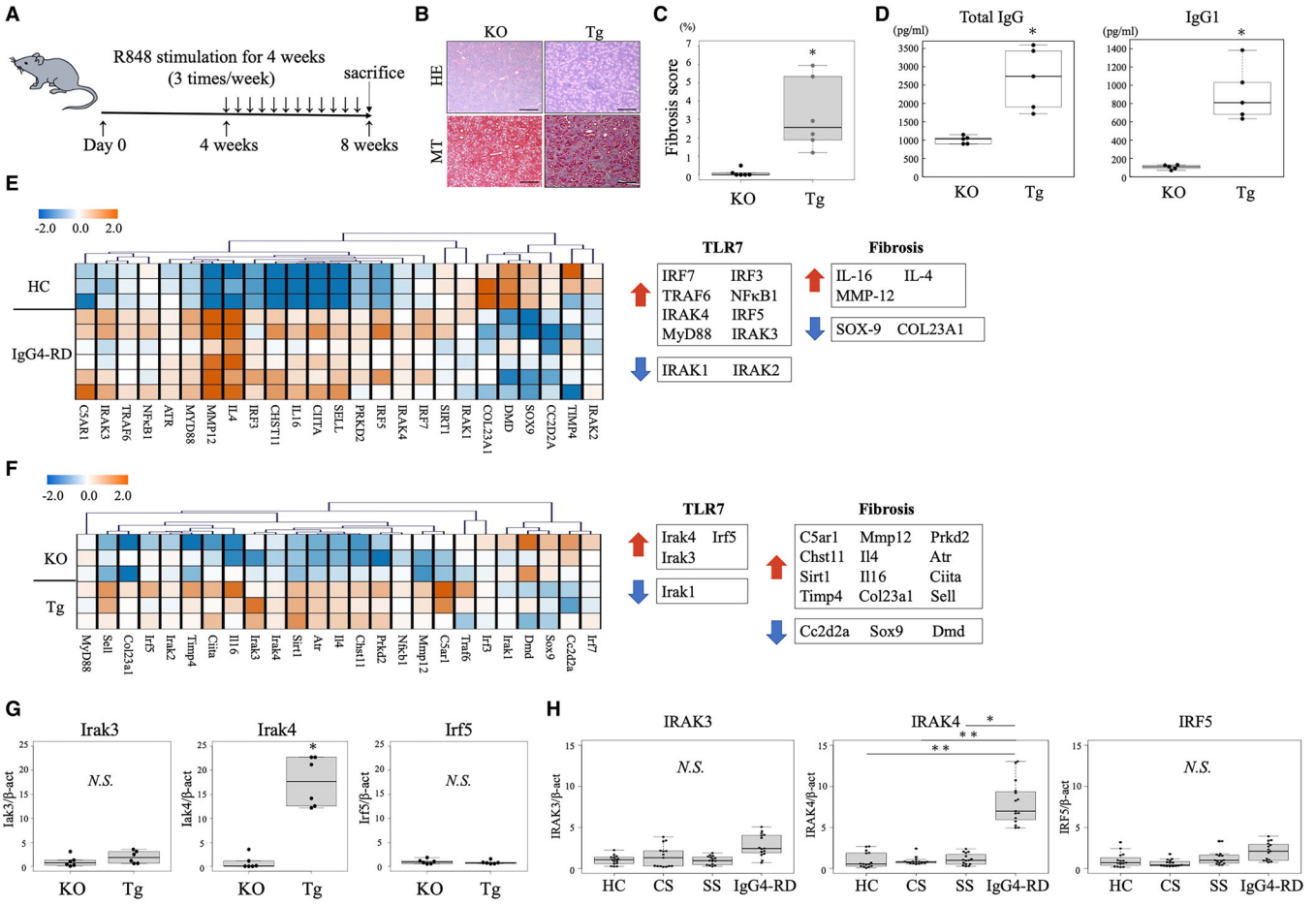

Figure 1. Toll-like receptor 7 (TLR-7)–related gene expression patterns in salivary glands (SGs) from patients with IgG4-related disease (IgG4-RD) and *TLR7*-transgenic/TLR-7$^{-/-}$ mice. **A**, Diagram of transgenic (Tg) and knockout (KO) mice before and after stimulation with the TLR-7 agonist R848. **B**, Hematoxylin and eosin (H&E)–stained and Masson's trichrome (MT)–stained sections of submandibular glands (SMGs) from representative mice. Bars = 100 μm. **C** and **D**, Fibrosis scores of SMGs (**C**) and serum IgG and IgG1 levels (**D**) in transgenic and knockout mice (n = 6 per group). **E** and **F**, Heatmaps showing differentially expressed TLR-7–related genes in SMGs from transgenic and knockout mice (**E**) and from IgG4-RD patients and healthy controls (HCs) (**F**). Only genes up-regulated or down-regulated ≥2-fold are shown. **G** and **H**, Expression levels of mRNA for TLR-7–related candidate genes in SGs from transgenic mice (n = 6) and knockout mice (n = 6) (**G**) and from healthy controls (n = 15), patients with chronic sialadenitis (CS) (n = 10), patients with Sjögren's syndrome (SS) (n = 15), and patients with IgG4-RD (n = 15) (**H**). In **C**, **D**, **G**, and **H**, data are shown as box plots. Each box represents the upper and lower interquartile range. Lines inside the boxes represent the median. Symbols represent individual subjects. * = $P < 0.05$; ** = $P < 0.01$, by Mann–Whitney U-test (**C**, **D**, and **G**) or Kruskal–Wallis test (**H**). NS = not significant.

genes was subsequently performed by increasing the number of cases.

Validation of TLR-7–related candidate genes in SGs. As shown in Figure 1G, the expression levels of mRNA for *Irak4* were significantly higher in SMGs from transgenic mice compared with those in knockout mice. Furthermore, the expression levels of mRNA for *IRAK4* were significantly higher in SGs from patients with IgG4-RD compared with those from the other groups, including patients with CS or SS and healthy controls (Figure 1H). The SG specimens were examined by immunohistochemistry to confirm the expression and distribution of TLR-7–related candidate molecules, including interferon regulatory factor 5 (IRF5), IRAK3, and IRAK4 (Supplementary Figure 3, available on the *Arthritis & Rheumatology* website at https://onlinelibrary.wiley.com/doi/10.1002/art.42043). Representative findings of IRAK4 are shown in Figures 2A and B. Based on morphologic identification, IRAK4 expression was detected in infiltrating inflammatory cells in the tissues from transgenic mice but not knockout mice (Figure 2A). In addition, the samples from patients with IgG4-RD showed enhanced infiltration of IRAK4-positive cells around ectopic GCs compared with those from patients with CS or SS and healthy controls (Figure 2B).

Because these control disease components are quite different from IgG4-RD, we examined the secondary lymphoid tissues of healthy controls. IRAK4 was detected at low levels around ectopic GCs in the tonsils of healthy controls but was frequently detected around the ectopic GCs in SMGs from patients with

IgG4-RD (Figure 2C). Moreover, the number of IRAK4-positive cells was significantly higher in IgG4-RD than in the other groups (Figure 2D).

Identification of IRAK4-expressing cells in SMGs. Because IRAK4 is mainly expressed in macrophages and dendritic cells (DCs) (25), SMG specimens from patients with IgG4-RD were stained for CD80 (marker for M1 macrophages), CD163 (M2 macrophages), CD11c (myeloid DCs), CD123 (plasmacytoid DCs), and IRAK4. The strong expressions of CD163+, CD11c+, and IRAK4-positive cells were observed in fibrotic areas and around ectopic GCs, whereas the minimal expressions of CD80+ and CD123+ cells were observed around the ectopic GCs (Figure 2E).

To identify the IRAK4-expressing cells in inflamed IgG4-RD tissues, SMG specimens from patients with IgG4-RD were stained with immunofluorescent antibodies to IRAK4, CD80, CD163, CD11c, CD123, and DAPI. We observed that many CD163+ cells were colocalized with IRAK4 in IgG4-RD tissues (Figure 2F). Furthermore, we performed quantitative analysis of the distributions of IRAK4-expressing CD80+, CD163+, CD11c+, or CD123+ cells in IgG4-RD tissues and found a significantly higher number of IRAK4-expressing CD163+ cells compared with other evaluated cells (Figure 2G).

Inflammatory cytokine production in M2 macrophages via TLR-7/IRAK4 signaling. We examined the effect of a TLR-7 agonist (loxoribine) and IRAK4 inhibitor (CA-4948) on

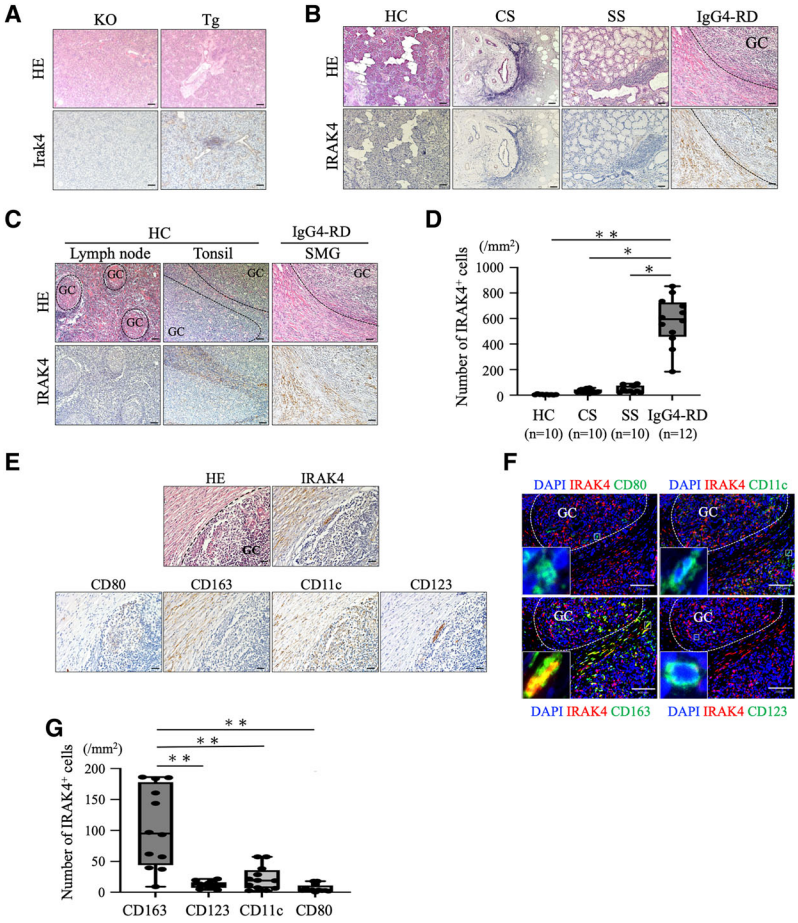

Figure 2. Identification and distribution of interleukin-1 receptor–associated kinase 4 (IRAK4) in SMGs from transgenic mice and patients with IgG4-RD. **A–C**, Distribution of TLR-7–related candidate molecules in SMGs from representative transgenic and knockout mice (**A**), from healthy controls and from patients with CS, SS, or IgG4-RD (**B**), and in tonsils and lymph nodes from healthy patients and SMGs from patients with IgG4-related dacryoadenitis and sialadenitis (IgG4-DS) (**C**). Outlined area indicates a germinal center (GC). Bars = 100 μm. **D**, Number of IRAK4-positive cells in SGs from healthy controls and patients with CS, SS, or IgG4-RD, measured using TissueQuest software. **E**, Serial sections stained with H&E or antibodies to IRAK4, CD80, CD163, CD11c, or CD123. Bars = 100 μm. **F**, Representative double immunostaining for IRAK4 (red), CD80 (green), CD163 (green), CD11c (green), and CD123 (green) in SMGs from patients with IgG4-RD. Counterstaining was performed with DAPI (blue). **G**, Number of IRAK4-expressing CD163+, CD123+, CD11c+, and CD80+ cells in SMGs from patients with IgG4-RD (n = 12), measured using TissueQuest software. In **D** and **G**, data are shown as box plots. Each box represents the upper and lower interquartile range. Lines inside the boxes represent the median. Symbols represent individual subjects. * = $P < 0.05$; ** = $P < 0.01$, by Kruskal–Wallis test. See Figure 1 for other definitions.

CD163+ M2 macrophages in vitro (Figure 3A). First, we confirmed the expression of TLR-7 in CD163+ M2 macrophages after differentiation and extraction, as described in the Patients and Methods section. The downstream pathways of TLR-7 are shown in Figure 3C. *MyD88, IRAK4, TRAF6,* and *NFKB* exhibited increased expression following treatment with the TLR-7 agonist, whereas *IRAK4, TRAF6,* and *NFKB* were down-regulated by the IRAK4 inhibitor (Figure 3D). Next, we determined the concentration of fibrotic cytokines (IL-33, IL-1β, and transforming growth factor β [TGFβ]) in culture supernatants in the presence or absence of the TLR-7 agonist and/or IRAK4 inhibitor. The concentrations of IL-33, IL-1β, and TGFβ in the culture supernatants were significantly increased after stimulation with the TLR-7 agonist. Furthermore, the concentrations of these cytokines were significantly decreased in the presence of the IRAK4 inhibitor (Figure 3E).

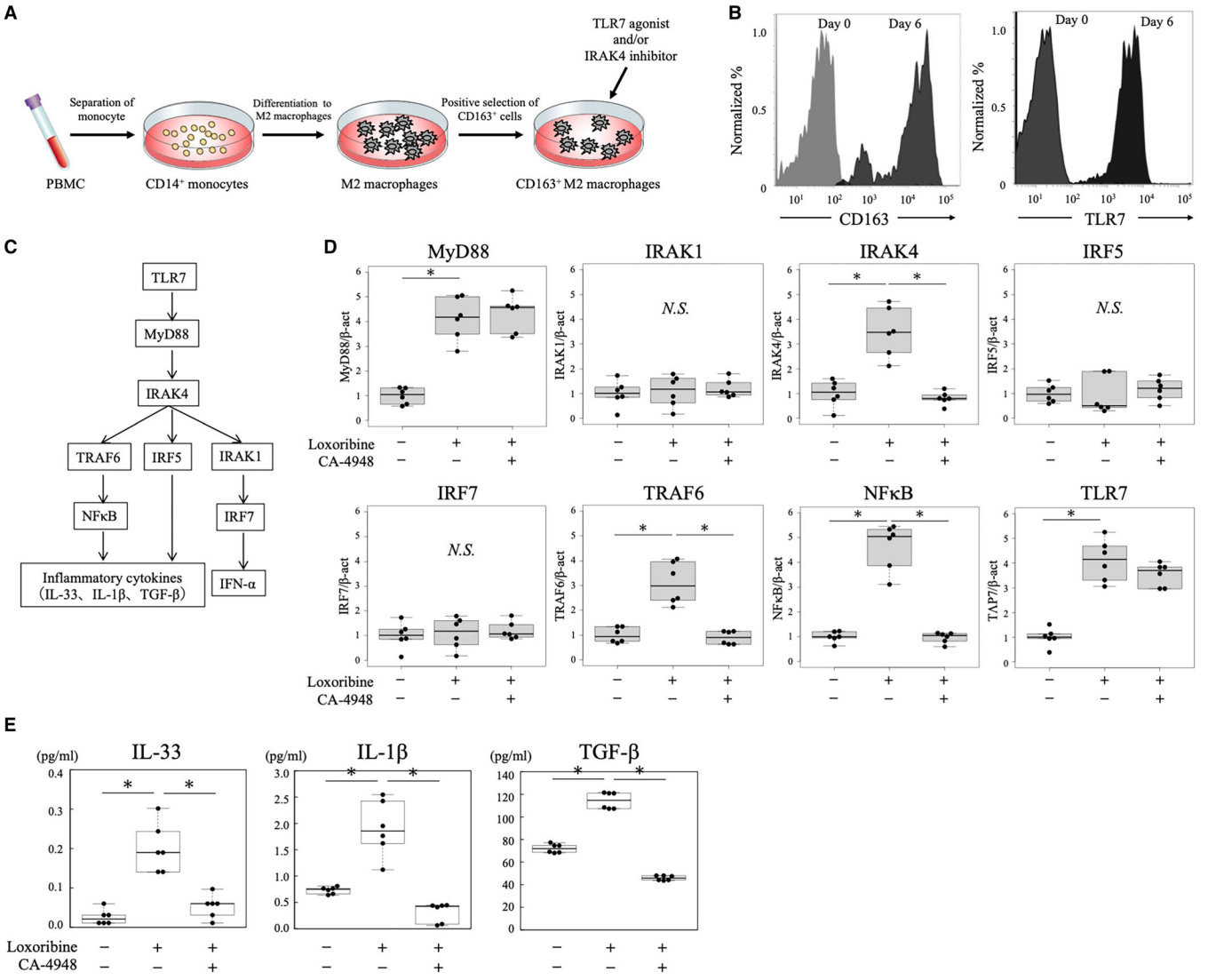

Figure 3. Expression of inflammatory cytokines and Toll-like receptor 7 (TLR-7)–related candidate genes in M2 macrophages. **A**, Schematic illustration of the extraction of human CD163+ M2 macrophages stimulated with the TLR-7 agonist loxoribine and/or interleukin-1 receptor–associated kinase 4 (IRAK4) inhibitor CA-4948. **B**, Detection of CD163 and TLR-7 before and after the differentiation and selection of M2 macrophages (day 0 and day 6) from ≥2 independent experiments, as determined by flow cytometric analysis. **C**, Schematic representation of TLR-7 pathways. **D**, Expression levels of mRNA for TLR-7–related genes in human CD163+ M2 macrophages cultured in the presence or absence of loxoribine and/or CA-4948 (n = 6 per group). **E**, Production of inflammatory cytokines in CD163+ M2 macrophages stimulated in the presence or absence of loxoribine and/or CA-4948, as determined by enzyme-linked immunosorbent assay. In **D** and **E**, Data are shown as box plots. Each box represents the upper and lower interquartile range. Lines inside the boxes represent the median. Symbols represent individual subjects. * = $P < 0.05$; ** = $P < 0.01$, by Mann–Whitney U-test (**D**) or Kruskal–Wallis test (**E**). PBMC = peripheral blood mononuclear cells; MyD88 = myeloid differentiation factor 88; TRAF6 = tumor necrosis factor receptor–associated factor 6; IRF-5 = interferon (IFN) regulatory factor 5; IL-33 = interleukin-33; TGFβ = transforming growth factor β; NS = not significant.

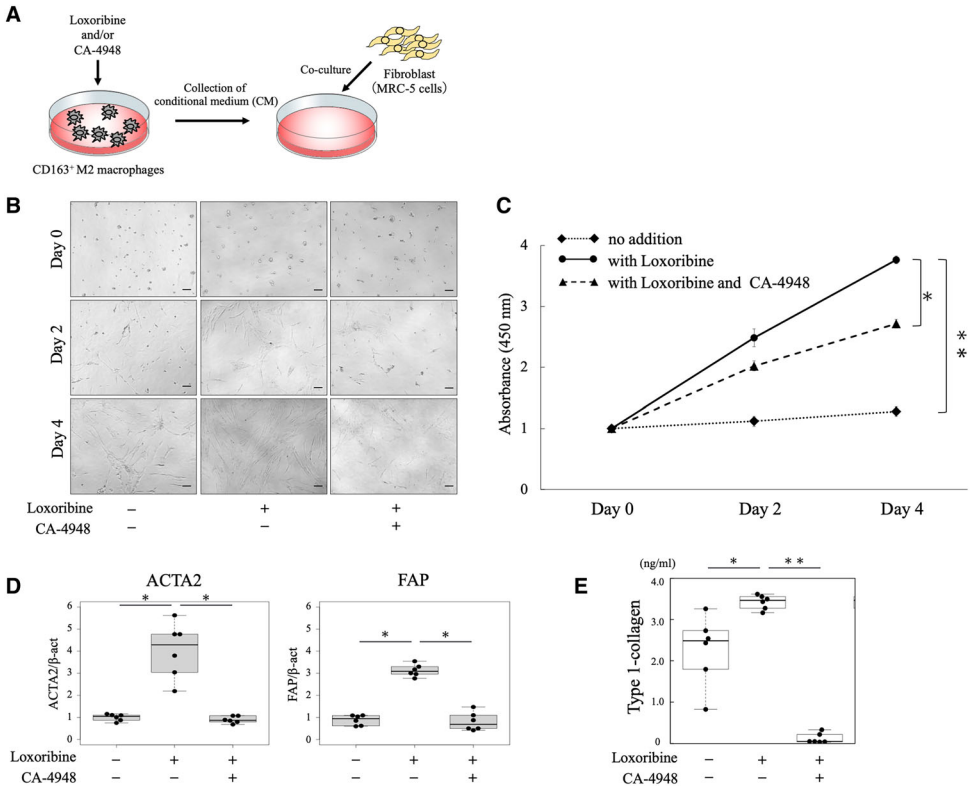

Figure 4. Involvement of M2 macrophages in the proliferation and activation of fibroblasts. **A**, Schematic illustration of the co-cultivation of human fibroblasts (MRC-5 cells) with conditioned medium derived from CD163+ M2 macrophages stimulated with loxoribine and/or CA-4948. **B**, Representative image of MRC-5 cells cultured in the conditioned medium derived from CD163+ cells in the presence or absence of loxoribine and/or CA-4948. Bars = 100 μm. **C**, Proliferation of MRC-5 cells cultured in the conditioned medium derived from of CD163+ cells in the presence or absence of loxoribine and/or CA-4948 (n = 6 per group). **D**, Expression levels of mRNA for fibrosis-related genes in MRC-5 cells in the presence or absence of loxoribine and/or CA-4948 (n = 6 per group). **E**, Production of type I collagen in MRC-5 cells stimulated in the presence or absence of loxoribine and/or CA-4948, as determined by enzyme-linked immunosorbent assay. Data are shown as box plots. Each box represents the upper and lower interquartile range. Lines inside the boxes represent the median. Symbols represent individual subjects.* = $P < 0.05$; ** = $P < 0.01$, by Kruskal–Wallis test.

Effect of the TLR-7 agonist and IRAK4 inhibitor on the proliferation and activation of fibroblasts. Because our recent data indicated that M2 macrophages might promote fibrosis in the local lesions from patients with IgG4-RD (13), we evaluated the in vitro response of fibroblasts (MRC-5 cells) to culturing in the conditioned medium derived from CD163+ cells

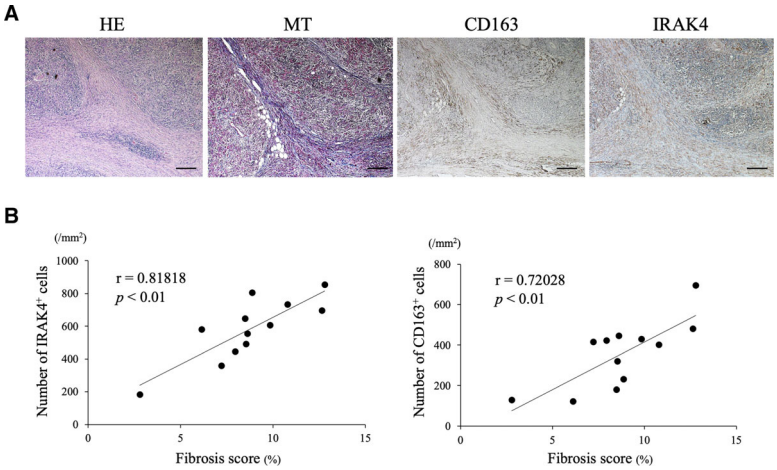

Figure 5. Correlation between fibrosis and M2 macrophages in SMGs from patients with IgG4-RD. **A**, Serial sections stained with H&E, MT, or antibodies to CD163 or interleukin-1 receptor–associated kinase 4 (IRAK4). Bars = 100 μm. **B**, Correlation between fibrosis score and the number of CD163+ or IRAK4-positive cells in SMGs (n = 12 per group). The numbers of CD163+ cells and IRAK4-positive cells were measured using TissueQuest software. Correlation coefficients and *P* values were determined using Spearman's rank correlation. See Figure 1 for other definitions.

treated with the TLR-7 agonist and/or IRAK4 inhibitor (Figure 4A). On day 4, a higher cell density was observed for fibroblasts cultured in the conditioned medium derived from CD163+ cells treated with the TLR-7 agonist compared with the conditioned medium alone or the conditioned medium treated with the TLR-7 agonist and IRAK4 inhibitor (Figure 4B). Next, we performed a cell proliferation assay, which indicated that cell viability in MRC-5 cells cultured in the conditioned medium derived from CD163+ cells treated with the TLR-7 agonist was significantly greater than that in the other conditioned media (Figure 4C). Additionally, a cell division assay revealed an increased cell division rate of MRC-5 cells cultured in the conditioned medium derived from CD163+ cells treated with the TLR-7 agonist compared with that in the other conditioned media (Supplementary Figure 4, available on the *Arthritis & Rheumatology* website at https://onlinelibrary.wiley.com/doi/10.1002/art.42043). Moreover, increased expression of *ACTA2* and *FAP* and higher type I collagen levels were detected in these cells (Figures 4D and E).

Evaluation of fibrosis scores in SMGs. Finally, we investigated the relationships between fibrosis scores and the number of IRAK4-positive or CD163+ cells in SMGs from patients with IgG4-RD. Specimens were stained with Masson's trichrome to evaluate the degree of fibrosis in the SMGs. The fibrosis scores determined by Masson's trichrome staining were defined as described in the Patients and Methods section. The tissues from IgG4-DS patients showed severe cordlike fibrosis and extensive ectopic GC formation (Figure 5A). The fibrosis score was positively correlated with the number of IRAK4-positive cells and CD163+ cells (Figure 5B).

DISCUSSION

IgG4-RD is pathologically characterized by the dense infiltration of lymphocytes/plasma cells, obliterative phlebitis, and marked fibrosis (termed "storiform fibrosis") (30). In particular, marked fibrosis often irreversibly impairs the functions of affected organs, such as the pancreas, kidneys, and lungs, in patients with diabetes mellitus, renal insufficiency, and interstitial pneumonia, respectively. Therefore, the elucidation of the fibrotic mechanism in IgG4-RD is essential for the prevention of organ dysfunction.

Recently, several studies demonstrated that innate immune cells such as basophils, plasmacytoid DCs, and M2 macrophages might be involved in the initiation and fibrosis of IgG4-RD (18–20) or the phenotypes of other mouse models (31,32) via TLR signaling. The dominant infiltration of basophils expressing TLR-2 and/or TLR-4 was shown in the pancreatic lesions of IgG4-related AIP (18). Notably, Watanabe et al suggested that interferon-α and IL-33 produced by plasmacytoid DCs promoted chronic fibro-inflammatory responses underlying the AIP model mouse and human IgG4-related AIP (33).

M2 macrophages (alternatively known as activated macrophages) are induced by IL-4 and are known to have a critical role in tissue repair and the progression of fibrotic diseases (34,35). Previously, we examined the involvement of M2 macrophages in

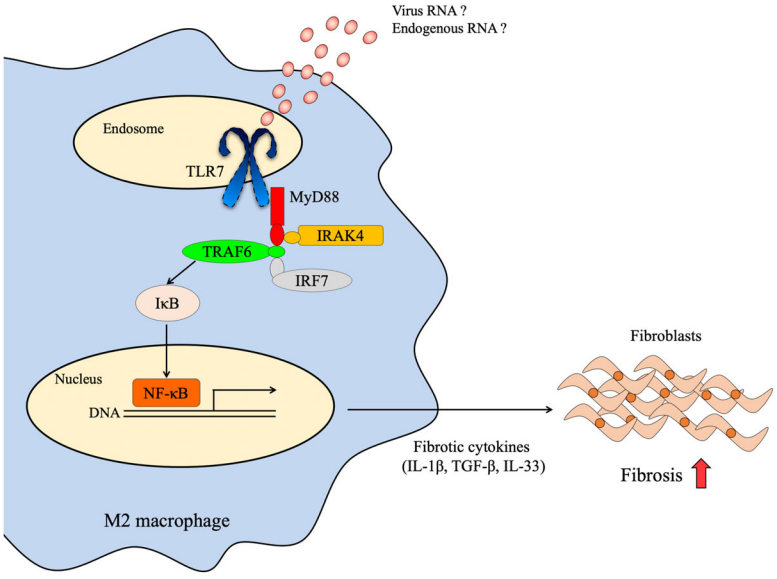

Figure 6. Schematic model of TLR-7 signaling in M2 macrophages leading to fibrosis in IgG4-RD. TLR-7 expressed on M2 macrophages recognizes some viral RNAs or self RNAs released from stressed or injured cells. Activated M2 macrophages secrete fibrotic cytokines, including interleukin-1β (IL-1β), transforming growth factor β (TGFβ), and IL-33, via interleukin-1 receptor–associated kinase 4 (IRAK4)/NF-κB signaling, which leads to fibrosis. MyD88 = myeloid differentiation factor 88; TRAF6 = tumor necrosis factor receptor–associated factor 6; IRF-7 = interferon regulatory factor 7 (see Figure 1 for other definitions).

the fibrosis of SMGs from patients with IgG4-RD, SS, and CS and indicated that the fibrosis score was positively correlated with the frequency of M2 macrophages in SMGs from IgG4-DS patients but not in those from the other groups (16). These results suggest that M2 macrophages might preferentially promote the fibrosis of affected lesions in IgG4-RD patients. In addition, our recent data demonstrated that TLR-7–expressing M2 macrophages may contribute to the fibrotic inflammation of affected organs via IL-33 secretion in IgG4-RD patients and *TLR7*-transgenic mice (22), but the details of the fibrosis mechanism in IgG4-RD via the downstream pathways of TLR-7 signaling remain unknown. TLR-7, mainly expressed on macrophages and DCs, recognizes several synthetic compounds and single-stranded RNAs of viruses. Ewald et al have suggested that TLR-7 recognizes exogenous and endogenous RNAs from damaged tissues or apoptotic cells and can contribute to the pathogenesis of autoimmune and allergic diseases (36). In this study, we performed differential expression analysis using DNA microarrays to investigate TLR-7–related molecules in the SMGs of *TLR7*-transgenic mice and IgG4-RD patients.

Microarray analysis of SMGs demonstrated significant increases in the TLR-7–related genes *IRF5, IRAK3*, and *IRAK4* in *TLR7*-transgenic mice and IgG4-RD patients. In addition, validation by quantitative real-time PCR and immunohistochemical staining revealed the overexpression of IRAK4 in SMGs from patients with IgG4-RD compared with the other groups. IRAK4 is a critical component of the TLR/IL-1 receptor signaling pathway and plays an important role in the innate immune system and inflammation (37,38). Moreover, Leah et al demonstrated that the inhibition of IRAK4 decreased the production of several inflammatory cytokines (IL-1β, IL-6, and tumor necrosis factor) in TLR-7 agonist (R848)–treated human monocytes via the activation of NF-κB (39). We confirmed that TLR-7–positive CD163+ M2 macrophages secreted IL-33, IL-1β, and TGFβ via TLR-7/IRAK4/NF-κB signaling pathways, which promoted the activation and proliferation of human fibroblasts in vitro (Figure 4). In addition, the fibrosis scores positively correlated with the number of CD163+ cells and IRAK4-positive cells in patients with IgG4-DS (Figure 5). The findings presented here confirm that CD163+ M2 macrophages promote the fibrosis of swollen lesions from IgG4-RD patients via IRAK4 signaling. Moreover, we previously reported the abundant infiltration of IL-1β–secreting and TGFβ1-secreting CD4+ cytotoxic T lymphocytes (CTLs) in the peripheral blood and inflammatory tissue lesions of IgG4-RD patients (7). These active cytokine–secreting effector CD4+ CTLs are linked to chronic inflammation and fibrosis.

In conclusion, based on the data reported here and published previously, a proposed model for the fibrotic mechanism in IgG4-RD is shown in Figure 6. TLR-7–expressing M2 macrophages in affected organs recognize some viral RNAs or self RNAs released from stressed or injured cells and promote the production of several fibrotic cytokines (IL-33, IL-1β, and TGFβ) via TLR-7/IRAK4/NF-κB signaling, which leads to severe fibrosis in affected organs. Thus, novel pharmacologic strategies that inhibit TLR-7 or IRAK4 might be applied to treat the inflammation and fibrosis of affected organs.

ACKNOWLEDGMENTS

We thank Takuma Shibata, PhD, Yuji Motoi, PhD, and Kensuke Miyake, MD, PhD, from the Division of Innate Immunity, Department of Microbiology and Immunology, Institute of Medical Science, University of Tokyo for their technical support, and Melissa Crawford, PhD, and J. Ludovic Croxford, PhD, from Edanz Group (https://jp.edanz.com/ac) for editing a draft of this manuscript.

AUTHOR CONTRIBUTIONS

All authors were involved in drafting the article or revising it critically for important intellectual content, and all authors approved the final version to be published. Dr. Moriyama had full access to all of the data in the study and takes responsibility for the integrity of the data and the accuracy of the data analysis.

Study conception and design. Chinju, Moriyama, Nakamura.

Acquisition of data. Moriyama, Kakizoe-Ishiguro, Haque, Sakamoto, Kibe, Ito-Ohta.

Analysis and interpretation of data. Chinju, Moriyama, Chen, Miyahara, Furusho, Kai, Hatakeyama-Furukawa, Maehara, Nakamura.

REFERENCES

1. Hamano H, Kawa S, Horiuchi A, Unno H, Furuya N, Akamatsu T, et al. High serum IgG4 concentrations in patients with sclerosing pancreatitis. N Engl J Med 2001;344:732–8.
2. Umehara H, Okazaki K, Masaki Y, Kawano M, Yamamoto M, Saeki T, et al. A novel clinical entity, IgG4-related disease (IgG4RD): general concept and details. Mod Rheumatol 2012;22:1–14.
3. Stone JH, Zen Y, Deshpande V. IgG4-related disease. N Engl J Med 2012;366:539–51.
4. Nirula A, Glaser SM, Kalled SL, Taylor FR. What is IgG4? A review of the biology of a unique immunoglobulin subtype. Curr Opin Rheumatol 2011;23:119–24.
5. Tanaka A, Moriyama M, Nakashima H, Miyake K, Hayashida JN, Maehara T, et al. Th2 and regulatory immune reactions contribute to IgG4 production and the initiation of Mikulicz disease. Arthritis Rheum 2012;64:254–63.
6. Maehara T, Moriyama M, Nakashima H, Miyake K, Hayashida JN, Tanaka A, et al. Interleukin-21 contributes to germinal centre formation and immunoglobulin G4 production in IgG4-related dacryoadenitis and sialoadenitis, so-called Mikulicz's disease. Ann Rheum Dis 2012;71:2011–19.
7. Maehara T, Mattoo H, Ohta M, Mahajan VS, Moriyama M, Yamauchi M, et al. Lesional CD4+ IFN-γ+ cytotoxic T lymphocytes in IgG4-related dacryoadenitis and sialoadenitis. Ann Rheum Dis 2017;76:377–85.
8. Tsuboi H, Matsuo N, Iizuka M, Tsuzuki S, Kondo Y, Tanaka A, et al. Analysis of IgG4 class switch-related molecules in IgG4-related disease. Arthritis Res Ther 2012;14:R171.
9. Zen Y, Fujii T, Harada K, Kawano M, Yamada K, Takahira M, et al. Th2 and regulatory immune reactions are increased in immunoglobin G4-related sclerosing pancreatitis and cholangitis. Hepatology 2007;45:1538–46.
10. Moriyama M, Tanaka A, Maehara T, Furukawa S, Nakashima H, Nakamura S. T helper subsets in Sjögren's syndrome and

IgG4-related dacryoadenitis and sialoadenitis: a critical review. J Autoimmun 2014;51:81–8.
11. Akiyama M, Suzuki K, Yamaoka K, Yasuoka H, Takeshita M, Kaneko Y, et al. Number of circulating follicular helper 2 T cells correlates with IgG4 and interleukin-4 levels and plasmablast numbers in IgG4-related disease. Arthritis Rheumatol 2015;67:2476–81.
12. Mattoo H, Mahajan VS, Della-Torre E, Sekigami Y, Carruthers M, Wallace ZS, et al. De novo oligoclonal expansions of circulating plasmablasts in active and relapsing IgG4-related disease. J Allergy Clin Immunol 2014;134:679–87.
13. Nakamura T, Satoh-Nakamura T, Nakajima A, Kawanami T, Sakai T, Fujita Y, et al. Impaired expression of innate immunity-related genes in IgG4-related disease: a possible mechanism in the pathogenesis of IgG4-RD. Mod Rheumatol 2020;30:551–7.
14. Uchida K, Okazaki K. Clinical and pathophysiological aspects of type 1 autoimmune pancreatitis. J Gastroenterol 2018;53:475–83.
15. Nakajima A, Masaki Y, Nakamura T, Kawanami T, Ishigaki Y, Takegami T, et al. Decreased expression of innate immunity-related genes in peripheral blood mononuclear cells from patients with IgG4-related disease. PLoS One 2015;10:e0126582.
16. Furukawa S, Moriyama M, Tanaka A, Maehara T, Tsuboi H, Iizuka M, et al. Preferential M2 macrophages contribute to fibrosis in IgG4-related dacryoadenitis and sialoadenitis, so-called Mikulicz's disease. Clin Immunol 2015;156:9–18.
17. Furukawa S, Moriyama M, Miyake K, Nakashima H, Tanaka A, Maehara T, et al. Interleukin-33 produced by M2 macrophages and other immune cells contributes to Th2 immune reaction of IgG4-related disease. Sci Rep 2017;7:42413.
18. Yanagawa M, Uchida K, Ando Y, Tomiyama T, Yamaguchi T, Ikeura T, et al. Basophils activated via TLR signaling may contribute to pathophysiology of type 1 autoimmune pancreatitis. J Gastroenterol 2018;53:449–60.
19. Yoshikawa T, Watanabe T, Minaga K, Kamata K, Kudo M. Cytokines produced by innate immune cells in IgG4-related disease. Mod Rheumatol 2019;29:219–25.
20. Watanabe T, Yamashita K, Fujikawa S, Sakurai T, Kudo M, Shiokawa M, et al. Involvement of activation of toll-like receptors and nucleotide-binding oligomerization domain–like receptors in enhanced IgG4 responses in autoimmune pancreatitis. Arthritis Rheumatol 2012;64:914–24.
21. Fukui Y, Uchida K, Sakaguchi Y, Fukui T, Nishio A, Shikata N, et al. Possible involvement of Toll-like receptor 7 in the development of type 1 autoimmune pancreatitis. J Gastroenterol 2015;50:435–44.
22. Ishiguro N, Moriyama M, Furusho K, Furukawa S, Shibata T, Murakami Y, et al. Activated M2 macrophages contribute to the pathogenesis of IgG4-related disease via Toll-like receptor 7/interleukin-33 signaling. Arthritis Rheumatol 2020;72:166–78.
23. Moriyama M, Furukawa S, Kawano S, Goto Y, Kiyoshima T, Tanaka A, et al. The diagnostic utility of biopsies from the submandibular and labial salivary glands in IgG4-related dacryoadenitis and sialoadenitis, so-called Mikulicz's disease. Int J Oral Maxillofac Surg 2014;43:1276–81.
24. Umehara H, Okazaki K, Kawa S, Takahashi H, Goto H, Mastui S, et al. The 2020 revised comprehensive diagnostic (RCD) criteria for IgG4-RD. Mod Rheumatol 2021;31:529–33.
25. Masaki Y, Sugai S, Umehara H. IgG4-related diseases including Mikulicz's disease and sclerosing pancreatitis: diagnostic insights. J Rheumatol 2010;37:1380–5.
26. Fujibayashi T, Sugai S, Miyasaka N, Hayashi Y, Tsubota K. Revised Japanese criteria for Sjögren's syndrome (1999): availability and validity. Mod Rheumatol 2004;14:425–34.
27. Shiboski CH, Shiboski SC, Seror R, Criswell LA, Labetoulle M, Lietman TM, et al, and the International Sjögren's Syndrome Criteria Working Group. 2016 American College of Rheumatology/European League Against Rheumatism classification criteria for primary Sjögren's syndrome: a consensus and data-driven methodology involving three international patient cohorts. Arthritis Rheumatol 2017;69:35–45.
28. Ohta M, Moriyama M, Maehara T, Gion Y, Furukawa S, Tanaka A, et al. DNA microarray analysis of submandibular glands in IgG4-related disease indicates a role for MARCO and other innate immune-related proteins. Medicine (Baltimore) 2016;95:e2853.
29. Moriyama M, Hayashida JN, Toyoshima T, Ohyama Y, Shinozaki S, Tanaka A, et al. Cytokine/chemokine profiles contribute to understanding the pathogenesis and diagnosis of primary Sjögren's syndrome. Clin Exp Immunol 2012;169:17–26.
30. Umehara H, Okazaki K, Kawa S, Takahashi H, Goto H, Matsui S, et al. The 2020 revised comprehensive diagnostic (RCD) criteria for IgG4-RD. Mod Rheumatol 2021;31:529–33.
31. Yamashina M, Nishio A, Nakayama S, Okazaki T, Uchida K, Fukui T, et al. Comparative study on experimental autoimmune pancreatitis and its extrapancreatic involvement in mice. Pancreas 2012;41:1255–62.
32. Haruta I, Yanagisawa N, Kawamura S, Furukawa T, Shimizu K, Kato H, et al. A mouse model of autoimmune pancreatitis with salivary gland involvement triggered by innate immunity via persistent exposure to avirulent bacteria. Lab Invest 2010;90:1757–69.
33. Watanabe T, Yamashita K, Arai Y, Minaga K, Kamata K, Nagai T, et al. Chronic fibro-inflammatory responses in autoimmune pancreatitis depend on IFN-a and IL-33 produced by plasmacytoid dendritic cells. J Immunol 2017;198:3886–96.
34. Sica A, Mantovani A. Macrophage plasticity and polarization: in vivo veritas. J Clin Invest 2012;122:787–95.
35. Alessandro V, Rama M, Hyejeong C, Andrew J, Jeffrey D, Debra L, et al. Characterization of distinct macrophage subpopulations during nitrogen mustard-induced lung injury and fibrosis. Am J Respir Cell Mol Biol 2016;54:436–46.
36. Ewald SE, Barton GM. Nucleic acid sensing Toll-like receptors in autoimmunity. Curr Opin Immunol 2011;23:3–9.
37. Picard C, Puel A, Bonnet M, Ku CL, Bustamante J, Yang K, et al. Pyogenic bacterial infections in humans with IRAK-4 deficiency. Science 2003;299:2076–9.
38. Suzuki N, Suzuki S, Duncan GS, Millar DG, Wada T, Mirtsos C, et al. Severe impairment of interleukin-1 and Toll-like receptor signalling in mice lacking IRAK-4. Nature 2002;416:750–6.
39. Cushing L, Winkler A, Jelinsky SA, Lee K, Korver W, Hawtin R, et al. IRAK4 kinase activity controls Toll-like receptor-induced inflammation through the transcription factor IRF5 in primary human monocytes. J Biol Chem 2017;292:18689–98.